A Study of Solar Flare Continuum Events Observed at Metre Wavelengths

R. D. Robinson

Sacramento Peak Observatory, Sunspot, New Mexico 88349, U.S.A.

Abstract

This paper presents observations and an interpretation of solar flare continuum radiation. Two types are distinguished: FCM which often precedes a moving type IV burst, and FCII which often follows a type II burst. Theoretical models are proposed for the two types of flare continuum event. For FCM events, the electrons are assumed to be injected into coronal arches, where they are confined by Coulomb scattering and wave–particle interactions. The radiation is due to either gyrosynchrotron or Langmuir wave processes. For FCII events, the electrons are assumed to be accelerated by large amplitude Alfvénic turbulence, the resultant radiation being caused by the conversion of Langmuir waves to electromagnetic radiation at the fundamental.

1. Introduction

The solar flare continuum is a long-lasting metre wavelength radiation. It is closely related to solar flares, but can be differentiated from a moving type IV by its 'stationary' position and from a stationary type IV by its temporal association with the flash phase of the flare. The term 'flare continuum' was first introduced by Wild (1970) and has been the subject of a short study by Robinson and Smerd (1975). It is identical, at least in some cases, to the broad-band continuum studied by Böhme (1972) and the $IVmA_1$ described by Krüger (1972) and Akin'yan (1972). These authors pointed out the coincidence often seen with microwave and type II bursts and the correlations found with high energy flare and proton events.

Flare continuum events fall into two basic classifications, shown schematically in Fig. 1. The first classification includes continuum starting at the flash phase of the event and usually accompanied by scattered weak groups of type III bursts. This continuum is often followed by a moving type IV event (I found a 70% association) and is therefore designated an FCM.

The second main type of flare continuum event is closely associated with type II bursts, always developing out of the trailing edge of the type II. I have termed this classification an FCII. Often the FCII shows properties similar to those of the stationary type IV, such as: stationary position, long duration, high polarization and a relatively structure-free continuum. However, the clear association with type II bursts and with the optical flare easily classifies the burst type. The type II–FC activity is occasionally accompanied by an unclassified continuum burst, sometimes having the properties of a type III–V event. Normally this unclassified continuum extends to microwave frequencies.

Table 1. Properties of observed flare continuum events

$S_{\geqslant 1\,GHz}(max)$ is the peak flux density of the microwave burst, $P(max)$ is the maximum circular polarization, while 1 s.f.u. (solar flux unit) = 10^4 Jy

Event occurrence	Frequency (MHz)	Event type	Start (UT) h m s	Duration h m	Flare imp.	$S_{\geqslant 1\,GHz}(max)^C$ (s.f.u.)	$T_b(max)$ (MK)	Ang. size (min^2)	$P(max)$ (%)
4 Sept. 1968	80	FCII(V)^A	00 32 30	>04 00	1N	250 L	500	65–112	100
21 Mar. 1969	80	FCM	01 36 00	00 19 (>02 30)^B	2N	1100 L	10000	80–125	0
21/2 Mar. 1969	80	FCM	00 30 00	00 28	–B	100 S	?	40	0
22 Mar. 1969	80	FCM	03 50 00	00 20	–N	10 S	?	25	0
23/4 Mar. 1969	80	FCM	23 30 00	>00 53	Probably behind limb	14 S	?	200→112 (after IV detach)	0
30 Mar. 1969	80	FCII	≤02 53 00	00 37	Behind limb	25000 L	100	225	0
26 Apr. 1969	80	FCII(IV)	23 13 00	00 07	2N	450 L	100	110±15	0
29 May 1969	80	FCM	00 21 30	00 06.5	1B	160 S	300	115–157	0
27 Sept. 1969	80	FCII	03 57 00	>01 23	3B	350 L	260	300–80	60
3 Oct. 1969	80	FCM	02 57 30	00 16	1N	265 M	?	100→50	0
17 Dec. 1969	80	FCM	00 38 00	00 12 (01 52)^B	2B	80 M	140	83±15	0
27/8 Feb. 1970	80	FCII(V)^A	23 35 00	02 30	1B	7000 M	15	160→30	80
12 Mar. 1970	80	FCM	03 11 00	00 19 (00 42)^B	2N	3800 M	40	60±8	90
13 Apr. 1970	80	FCII(V)^A	04 20 30	>00 20	–B	80 S	90	235→142	0
15 Apr. 1970	80	FCII	04 29 00	00 30	2B	3000 L	?	190–125	20
17 Apr. 1970	80	FCM	01 31 00	00 16	–B	63 M	2	85	0
29 Apr. 1970	80	FCM	01 03 00	00 07 (00 30)^B	2N	20 L	500→100 (after IVm)	95±12→43±8 (after IVm)	0

Table 1 (*Continued*)

Event occurrence	Frequency (MHz)	Event type	Start (UT) h m s	Duration h m	Flare imp.	$S_{\geq 1\,\text{GHz}}$(max)[c] (s.f.u.)	T_b(max) (MK)	Ang. size (min²)	P(max) (%)
22 May 1970	80	FCII	00 36 30	03 30	None (disc event)	13 L	1500	118→70	90
30 July 1970	80	FCII	01 18 00	>02 40	1N	4 L	350	66–51	60
10/11 Aug. 1970	80	FCM	23 41 00	00 29	–N	None	?	120±11	0
26 Sept. 1970	80	FCII(V)[A]	00 27 00	01 01	2B	18 M	100	86→55	50
3 Dec. 1970	80	FCM	04 16 45	00 23	None (limb event)	100 S	1700	70–150	0
14 Sept. 1971	80	FCII	23 46 00	00 10	–N	30 L	70	100±15	0
23 Jan. 1972	80	FCM	23 19 00	00 18	–B	85 S	1000	42→165	0
22 Feb. 1972	80	FCII(V)[A]	00 46 00	>03 00	2N	1700 S	1500	55→28	80
26 Aug. 1972	160	FCII(V)[A]	03 44 30	00 50	None (limb event)	14 S	400	45±15→21±8	0
	80		03 55 30	00 40	None (limb event)	14 S	260	265→70	0
30 Aug. 1972	160	FCM	<04 36 30	>00 45	None (disc event)	None	40	28±8	0
	80		<04 36 30	>00 45	None (disc event)	None	80	70–85	0
28 Nov. 1972	160	FCII	04 18 00	00 32	1N	25 L	15	45	?
	80		04 18 00	00 32	1N	25 L	300	200–100	50
1 May 1973	160	FCII	02 50 00	>00 30	–B	5000 L	190	40–120	?
	80		02 57 00	>00 30	–B	5000 L	400	340–88	?
26 June 1973	160	FCM	01 35 00	00 10	–B	500 L	700	47±10	0
				(>01 30)[B]					
	80		01 37 00	00 08	–B	500 L	7000	140–185 [No. 1]	0
				(>01 30)[B]				180–220 [No. 2]	
4 June 1974	160	FCII(V)[A]	00 12 30	>00 30	1B	70 L	200	27±10	0
	80		00 26 30	>00 30	1B	70 L	40	150–80	50
6 Nov. 1974	160	FCII(V)[A]	03 14 30	00 56	1B	150 M	100	27–55	10
	80		03 26 00	00 54	1B	150 M	150	146–80	10

[A] This FCII event was accompanied by a V-like continuum.

[B] Times given in parentheses are durations of possible type IV events following the moving type IV. Such events may also be continuations of the flare continuum.

[C] Duration of microwave bursts is designated: S, short (<5 min.); M, medium (between 5 and 15 min.); L, long (>15 min.).

An observational study of the flare continuum was undertaken using data collected by the Division of Radiophysics, CSIRO. A total of 32 events was studied. For all events a dynamic spectrum was obtained covering frequencies from 10 to at least 2000 MHz. Unfortunately the continuum for many events was not detected on these spectra because of the low sensitivity of the instrument.

Single-frequency observations of the two-dimensional source properties were obtained by the Culgoora radioheliograph (Sheridan *et al.* 1972). Of the 32 events studied, 25 were observed exclusively at 80 MHz, 5 were seen at 160 and 80 MHz, and 2 were observed at 160, 80 and 43 MHz. A complete description of these events has been presented by Robinson (1977). A summary of the properties of each of the events is presented in Table 1. A summary of and comparison between the general characteristics of the FCM and FCII classifications is as follows:

Occurrence. The FCM occurs at the flash phase of the flare, the 80 and 160 MHz sources appearing simultaneously. The FCII occurs after a type II burst, the 160 MHz source appearing before the 80 MHz source.

Duration. The FCM lasts from 15 to 45 min. The FCII lasts from 20 min, to 4 h, the 160 MHz source fading before the 80 MHz source.

Dimensions. The average solid angle of the FCM is 86 min^2 arc at 80 MHz and 47 min^2 arc at 160 MHz. The area changes randomly with time for both 80 and 160 MHz sources. The average solid angle of the FCII is 47 min^2 arc at 80 MHz and 38 min^2 arc at 160 MHz. At both 80 and 160 MHz, the area of the source decreases with time.

Polarization. The FCM source is unpolarized at all times. The FCII source has values of circular polarization in the range 0–100%, increasing from 0% after about 15 min.

Structure. The source structure of both FCM and FCII events is arch-like (see Fig. 2).

Brightness. For FCM events, T_b varies from 5×10^7 to 5×10^9 K for both 80 and 160 MHz sources. For FCII events, T_b varies from 5×10^7 to 5×10^8 K for both 80 and 160 MHz sources.

Motions. The motions of FCM sources are random. For FCII sources, there are occasional outward motions, the average shift being about 5 min arc.

Associations. Both FCM and FCII events have 100% associations with flares and with microwave activity.

2. Flare Continuum Event

Low frequency (<40 MHz) continuum radiation was generally not observed on the dynamic spectrum and was also absent in those two events for which radioheliograph observations at 43 MHz were available. The sources were also long lasting, reasonably stationary and often showing an arch-like structure when observed simultaneously at 80 and 160 MHz (see Fig. 2). For these reasons I postulate that the source is produced in relatively low-lying coronal arches. The radiation mechanism and the means by which nonthermal electrons are confined and evolve in this arch are examined below.

(a) Radiation processes

Gyrosynchrotron Radiation

Synchrotron radiation processes have been postulated as the mechanism for one flare continuum event (Kai 1975). If the particle distribution function is a steeply decreasing function of energy, or if the nonthermal particles are located well above
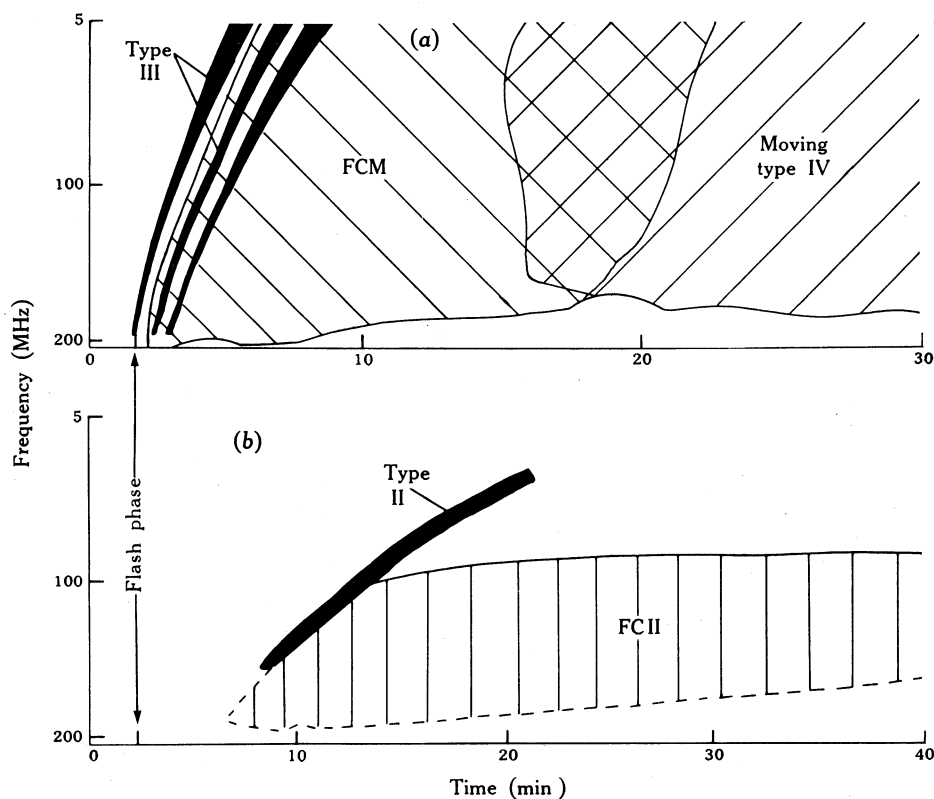

Fig. 1. Schematic representations of (a) FCM and (b) FCII events.
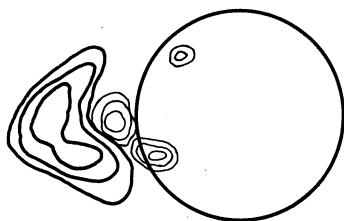

Fig. 2. Contours at 80 MHz (bold) and 160 MHz (light) of the FCM event of 30 August 1972. The contour spacing is $2^{-\frac{1}{4}}$ of the maximum brightness temperature at each frequency. The event shows a definite arch structure.

the coronal plasma level, then the synchrotron process is the only mechanism possible. Unfortunately, we have no direct information on the particle distribution function. While microwave observations suggest that power-law energy distributions are produced in flare acceleration processes, the confinement of these particles in a coronal arch may drastically alter the distribution. Furthermore, in most cases, observational evidence suggests that the flare continuum sources are located near

the type III heights. This does not allow us to differentiate between plasma and synchrotron processes without independent measurements of coronal magnetic fields and densities.

The most important information concerning emission processes comes from circular polarization observations. All FCM events began near the flash phase of the flare and were unpolarized during their entire lifetime. The synchrotron process can explain this low degree of polarization provided the magnetic field directions were randomized or the source was optically deep (Robinson 1974).

A randomization of field directions requires large-scale magnetic turbulence within the arch structure. This turbulence could be generated by the flare, but would play no role in the initial phase of the FCM event. This is because the turbulence travels at the Alfvén velocity and would require 5–10 min to reach the 80 MHz plasma level, whereas the FCM events start within a few seconds of the flash phase at all frequencies.
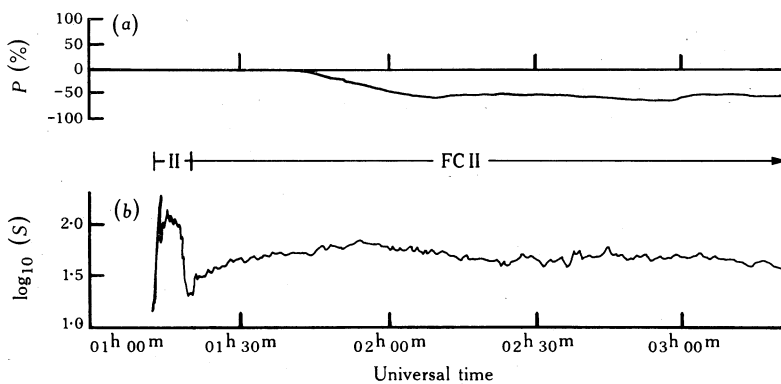

Fig. 3. Time evolution of (a) the circular polarization P and (b) the flux density S in arbitrary units for a typical FCII event (30 July 1970).

While an optically thick source produces low polarization, it also results in a brightness temperature which is nearly independent of the magnetic field or the number density of nonthermal particles. As the source fades it must become optically thin, which will result in an increase in polarization (Robinson 1974). All FCM events that were associated with the moving type IV disappeared in the interaction with the moving type IV, and polarization information during the fading is unavailable. However, those FCM bursts that were not associated with a moving type IV did *not* increase in polarization while fading, and they cannot be produced by synchrotron processes unless appreciable turbulence is generated before fading occurs.

FCII sources are often observed to increase in polarization while the brightness temperature is constant or increasing (see Fig. 3). After reaching a constant level, the polarization generally remains at this level ($\pm 10\%$) while the burst fades. This behaviour is incompatible with synchrotron radiation, where the increase in polarization occurs during the decaying phase of the burst, when the source is decreasing in optical depth. Furthermore, high circular polarizations ($> 80\%$) are sometimes seen to be accompanied by large brightness temperatures ($> 10^9$ K). For gyrosynchro-

tron radiation, however, a large polarization is generally associated with low energy electrons and small harmonic numbers (Kai 1969) and is generally incompatible with high brightness temperatures.

Centre-to-limb variation in maximum FCII source polarization (Fig. 4) shows high polarization except for very large observation angles or short-lived events, where depolarization effects may operate. This consistently high circular polarization is not seen in moving type IV bursts (a known synchrotron source) and is further evidence against synchrotron radiation being important in FCII events. We therefore conclude that while the gyrosynchrotron mechanism may produce the FCM (especially those associated with a moving type IV) it is unlikely to be important in the FCII.
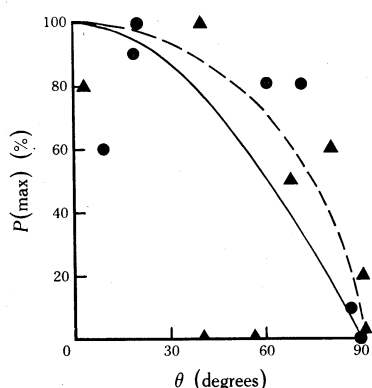

Fig. 4. Measurements at 80 MHz of the maximum circular polarization $P(\text{max})$ as a function of the observation angle θ, derived from the location of the associated optical flare. Solid and dashed curves represent $\cos\theta$ and $\cos^{\frac{1}{2}}\theta$ dependences. The triangles and circles represent events lasting shorter and longer than 15 min respectively.

Plasma Radiation

As seen from Table 1, flare continuum sources often correspond to brightness temperatures of less than 10^9 K. At these temperatures, plasma radiation will be emitted primarily at the fundamental (Melrose 1974a). Fundamental radiation, emitted from a region containing nonturbulent magnetic fields, may reach high degrees of polarization. We must therefore explain the low polarizations observed if plasma radiation is assumed to be the emission mechanism for the flare continuum event.

In subsection (b) below I present an FCII source model in which the radiation is produced by particles accelerated by large-scale magnetic turbulence, generated either by the associated type II shock or by reconnection processes generating the associated Hα flare. Such turbulence randomizes the magnetic field directions and thereby depolarizes the source. The decay or loss of the turbulence from the arch will then result in an increase of polarization. The polarization reaches a constant level, dependent upon observation angle and source properties, when the turbulence is totally absent. This seems to be the most probable explanation for the FCII.

There are three processes by which unpolarized plasma emission can be produced in an FCM: (i) Unpolarized second harmonic radiation is possible for bursts with observed brightness temperatures greater than 10^9 K, but is unlikely to dominate the fundamental for weaker events. (ii) Unpolarized radiation may result from an isotropic or nearly isotropic gap distribution in a weak magnetic field region (Robinson 1978b, present issue pp. 547–60); this process is always associated with brightness temperatures less than 5×10^8 K. (iii) Strong QT mode coupling near the plasma level by small-scale density inhomogeneities may depolarize the source; this was used by Melrose (1975a) to explain the low polarizations in type III bursts and

was suggested by Robinson (1978c) as a possible means of explaining the low polarization of type V events.

Melrose (1975a) speculated that the density inhomogeneities form principally in open field lines and are absent in coronal arches. He used the strong polarizations observed in stationary type IV sources and type I storms as evidence for this view. It is possible, however, that density inhomogeneities are absent only in strong magnetic arches and that they may still form if the magnetic strength is small enough. Thus, while the type I storm and the FCII may originate in strong field arches, the FCM would be created in a weak arch system.

Any of the three explanations of unpolarized radiation is possible and more detailed experimental information must become available before a definite choice can be made. In conclusion we may say that plasma emission at the fundamental is the most likely radiation mechanism for the FCII. A less definite statement can be made about the mechanism for the FCM. For most of the FCM events, models based upon either synchrotron or plasma wave processes will pattern the observed properties of the burst. It is my belief that in many events both processes play a role.

(b) Particle confinement and acceleration in arch

Model for FCM

FCM bursts have a strong temporal and positional correlation with weak groups of type II bursts occurring in the initial phases of the flare event. I propose that the nonthermal electrons responsible for the continuum radiation are accelerated during and after the flash phase of the flare and are trapped in the overlying coronal arches. The type III bursts are evidence for this injection process.

As the electron streams move along the magnetic fields they will be scattered. The leading electron streams are scattered by Coulomb interactions and the later ones by the hydromagnetic (HM) waves generated by their streaming motion (Melrose 1974b). Whistlers and HM waves will also be generated in the flare reconnection processes. These may become trapped in the loops and aid in particle confinement.

Particles confined in a magnetic mirror (i.e. a coronal arch) have a loss cone anisotropy. Such an anisotropy is highly unstable towards whistler production (Robinson 1977) and the level of whistler mode waves rapidly increases. This will affect the particle distribution in two ways:

Firstly, low energy particles resonate with the whistlers and will be scattered into the mirror loss cone. This causes an exponential loss of these low energy particles from the mirror system. The high energy particles, interacting with HM waves, require an extremely large anisotropy before they are appreciably affected (Robinson 1977). These particles are scattered primarily by Coulomb collisions and will be retained for a long period of time.

Secondly, low energy particles accelerated after the flash phase will be highly scattered by the whistler and will be rapidly thermalized. The result is a high energy filter which allows the buildup of energetic particles.

The combination of both processes, in conjunction with Coulomb scattering, results in a depletion of low energy electrons and may lead to an energy inversion ($\partial f/\partial E > 0$) in some range of the electron distribution. This results in bright plasma-wave emission (Robinson 1978b). It is probable that the effectiveness of the filtering process can vary appreciably, leading to the wide variation in brightness temperatures observed.

The relationship between the FCM and the moving type IV is not well understood and requires more theoretical and observational study. Quantitatively I believe that the most likely interaction is that proposed by Kai (1975) and Robinson and Smerd (1975) who postulated that the moving type IV source is produced within the FCM source region and absorbs many of the energetic electrons. For some events the moving type IV might disrupt the arch system, causing the rapid disappearance of the flare continuum. In many cases, however, the arch may remain intact and be the site of the late stationary type IV (or a continuation of the flare continuum).

Model for FCII

The FCII appears at a given frequency immediately following the associated type II burst. In the following model I postulate that the nonthermal electrons responsible for this radiation are produced by a stochastic acceleration process in which particle scattering by whistlers and high frequency Alfvén waves causes a transfer of energy from low frequency magnetic turbulence to the particles.

The waves responsible for the scattering are generated by particle pitch-angle anisotropies produced by the turbulence (see Melrose 1974b; Robinson 1977). The low frequency turbulence (probably in the form of Alfvén waves) may be produced by magnetic field reconnection at the time of the flare and then propagated in the enhanced fields above the active region at nearly the same velocity as the type II disturbance. Alternatively, the shock may induce the field fluctuations by exerting forces on the arch system (see e.g. Rosenberg 1970). Occasionally these processes induce large-scale standing waves within the arch and produce the pulsations sometimes seen during the flare continuum (McLean and Sheridan 1973).

The theory predicts a systematic acceleration rate v_A given by Melrose (1974b) as

$$v_A = \tfrac{1}{4}\pi\omega\varepsilon^2\beta_A/\beta \qquad \text{for} \qquad \beta > 43\,\beta_A, \tag{1a}$$

$$= 0 \qquad\qquad\qquad \beta < 43\,\beta_A, \tag{1b}$$

where $\varepsilon = B_t/B_0$ is the relative amplitude of the turbulence (with B_0 the background magnetic field strength and B_t the turbulent field strength at maximum), while ω is the frequency of the turbulence, $\beta = v/c$ is the dimensionless velocity of the resonant particle and $\beta_A = v_A/c$ is the dimensionless Alfvén velocity. A description of the formula (1) and its restrictions has been given by Robinson (1977). The low energy limit to the acceleration v_A is determined by the lowest energy for which whistler mode waves can interact with and scatter particles.

In addition to systematic acceleration, calculations indicate that there is also considerable diffusion in energy. This diffusion acts to smooth the energy gradients, and results in the formation of a nearly level energy distribution from low energies to a high energy cutoff E_m. While the value of E_m depends somewhat on the diffusion in energy, a rough estimate can be obtained by just using the systematic acceleration term along with the acceleration rate (1). This gives

$$\mathrm{d}E/\mathrm{d}t = v_A E, \tag{2}$$

so that we have

$$E_m(t) = (E_i^{1/2} + 2^{-3/2} A t E_0^{1/2})^2 \qquad \text{for} \qquad E_m \ll E_0 \tag{3a}$$

$$= E_0 \exp\big(A(t-t_0)\big) \qquad\qquad E_m \gtrsim E_0, \tag{3b}$$

where E_i is the energy of particles having $\beta = 43\beta_A$, $E_0 = m_0 c^2$ is the rest mass energy of the electron, $A = v_A \beta$ and t_0 is the time necessary to accelerate particles from E_i to E_0. As mentioned above, the radiation from an FCII source is most likely to be produced by Langmuir radiation. The large-scale turbulence responsible for electron acceleration will also act to depolarize the source. As this turbulence is damped or lost from the trap, the polarization rises, reaching a maximum steady value when the turbulence is completely absent.

Observations of polarization characteristics indicate that turbulence is trapped in the FCII source region for an average of 25 min. Using this as the acceleration time in equation (3) we find that, on the average, particles are accelerated to energies of 300–500 keV. The damping of these particles through Coulomb collisions determines the maximum lifetime of the burst.

Using the Coulomb collision formula of Benz and Gold (1971) we can estimate the rate of energy loss for electrons in the range $0\cdot1 < E_k < 10$ MeV within a completely ionized plasma as

$$dE_k/dt = (6\cdot3\pm1\cdot0)\times10^{-13} N \quad \text{MeV s}^{-1}, \tag{4}$$

where N is the number density of thermal ions present.

Weiss and Stewart (1965) calculated average number densities of particles trapped in a dipole field and found that for particles reaching the 40 MHz plasma level the average number density is $\bar{N} = 3\times10^8$ cm^{-3}. Putting this value into equation (4) yields a decay rate of about 200 eV s^{-1}. Hence, a particle having an energy of 300 keV will require 17 min to decay to 100 keV, where equation (4) is no longer valid, and will take only a few more minutes to decay to the thermal level. This is sufficiently long to explain the lifetime of most of the events observed. Longer lifetimes would be obtained for a higher frequency of turbulence or a stronger magnetic field. The degree of acceleration and the maximum energy will, however, be limited through plasma processes, such as quasilinear diffusion, and by the amount of energy available in the turbulence.

To understand the time behaviour of the source brightness, it is necessary to study the variation in the Langmuir wavenumber spectrum. This spectrum is produced by the nonthermal particles and will be converted to observational radiation either by scattering on electron clouds surrounding ambient ions or by the coalescence of two waves (see e.g. Tsytovich 1967, 1970; Melrose 1974a; Robinson 1977, 1978a).

In the formation of the spectrum by a plateau energy distribution the collisional damping at wavenumber k can be neglected by comparison with the reabsorption of the waves by the nonthermal particles, provided that the number density N_p of energetic particles satisfies the relation (Robinson 1978a)

$$N_p > 10^4 \gamma^3 k^3 v_m^3/c^3. \tag{5}$$

Here v_m specifies the high velocity cutoff of the plateau distribution. If this relation is satisfied for all wavenumbers then the Langmuir-wave brightness temperature spectrum is given as (Robinson 1978a)

$$KT_b(k) = (p_m^2 - p_\phi^2)/m_e, \tag{6}$$

where $p_m = \gamma_m m_e v_m$ and $p_\phi = m_e v_\phi$, while v_ϕ is the phase velocity of the wave. In

most cases p_ϕ is much less than p_m, so that Langmuir brightness temperatures can be expressed as

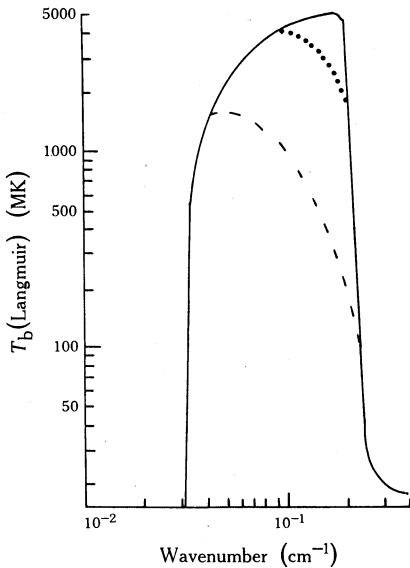$$KT_b(k) \approx \gamma^2 \beta_m^2 m_e c^2 . \qquad (7)$$

Fig. 5. Numerically calculated distributions of the Langmuir brightness temperature as a function of the wavenumber for a plateau energy distribution with a high energy cutoff at 100 keV. The assumed plasma frequency is 100 MHz. Spectra are for nonthermal electron number densities of 100 cm^{-3} (solid), 10 cm^{-3} (dotted) and 1 cm^{-3} (dashed curves).

Fig. 6. Distribution of the fundamental brightness temperature at 100 MHz as a function of the number density of nonthermal electrons for an assumed plateau energy distribution with a high energy cutoff at 100 keV. Associated Langmuir wavenumber spectra are shown in Fig. 5.

The plasma wave spectrum (and therefore the observed radiation) will rapidly increase in brightness temperature during the initial phase of the acceleration and will only slowly increase as the electrons become relativistic. This accounts for the rapid rise and the plateau of the observed flux in FCII events (as shown in Fig. 3).

After the acceleration has ceased, the energetic particles will decay in energy through Coulomb collisions and will be lost through the ends of the arch after interacting with the whistlers. As seen from the relation (7) the observed brightness temperature is

independent of the number density and is only slightly dependent upon the energy of the nonthermal particles, provided that the plateau extends to at least mildly relativistic energies and the number of nonthermal particles satisfies the relation (5). When the number density decreases to the point where the inequality (5) fails, damping will play a role in determining the Langmuir wavenumber spectrum. The brightness temperature at large wavenumbers will be considerably reduced (see Fig. 5) and the brightness of the observed radiation will decrease. Since the wave range over which the Langmuir temperature is reduced depends on the density of the nonthermal particles through the inequality (5), the observed brightness temperature will become highly dependent upon the number density (see Fig. 6). The rate of decay will then be determined by the rate at which the particles are lost from the confining region.

3. Conclusions

I have been able to explain the major features of solar flare continuum bursts. Basically, both types of flare continuum involve radiation from nonthermal particles accelerated near the start of the flaring event and confined within coronal arches. Most FCM events can be explained by either plasma or synchrotron radiation processes. The occasional observation of extremely intense FCM bursts, however, indicates induced plasma-wave emission. This implies that a well-developed 'gap' distribution of nonthermal electrons is produced for these events.

The FCM model, based on the strong temporal and positional correlation between type III bursts and the FCM, postulates that the nonthermal electrons are accelerated in the flare region and injected into a coronal arch. The particles are then confined in a mirror system and affected by Coulomb pitch-angle scattering and wave–particle interactions. Large energy densities of whistlers are generated by the loss cone anisotropy of the particles within the arch. These waves reduce the number of low energy particles by scattering these particles into the loss cone. They also act as a high energy filter for the electrons injected after the initial flash phase. These two processes, in conjunction with Coulomb collisions, may result in the formation of an energy inversion. The form of this inversion, the total number of high energy particles confined and the magnetic field strength will determine whether synchrotron or plasma-wave emission will dominate, as well as determine the brightness temperature observed.

Polarization information gives strong evidence that plasma-wave processes are the dominant emission mechanism for the FCII events. The FCII model postulates that nonthermal particles are accelerated further by large amplitude hydromagnetic turbulence, generated by either the reconnection process giving rise to the associated type II or by the type II shock itself. This acceleration is controlled by wave–particle scattering processes and will be effective only for those energies at which these processes are strong. For this reason there will be a rapid decline in the acceleration rate for velocities less than $43 v_A$. Because of the relatively large amount of diffusion in energy, a nearly level energy distribution will be produced.

As long as the magnetic turbulence is strong within the arch, the nonthermal particles will be accelerated. The observations indicate that the turbulence lasts about 25 min and theory predicts that energies up to 300–500 keV or more are obtained, depending upon the acceleration parameters. Particle losses through the ends of the loop system and Coulomb collisions with the ambient plasma determine the decay of the event. In addition to accelerating the particles the turbulence acts to randomize

field directions and depolarize the source. As the turbulence is lost the polarization increases, reaching a maximum when the turbulence is completely absent. The degree of polarization is independent of observed brightness and will remain constant as the burst fades. This patterns the observed behaviour.

Acknowledgments

References

Akin'yan, S. T. (1972). *Sov. Astron. AJ* **16**, 469.
Benz, A. O., and Gold, T. (1971). *Solar Phys.* **21**, 157.
Böhme, A. (1972). *Solar Phys.* **24**, 457.
Kai, K. (1969). *Proc. Astron. Soc. Aust.* **1**, 189.
Kai, K. (1975). *Solar Phys.* **45**, 217.
Krüger, A. (1972). 'Physics of Solar Continuum Bursts' (Akademie: East Berlin).
McLean, D. J., and Sheridan, K. V. (1973). *Solar Phys.* **32**, 485.
Magun, A., Stewart, R. T., and Robinson, R. D. (1975). *Proc. Astron. Soc. Aust.* **2**, 367.
Melrose, D. B. (1974a). *Solar Phys.* **35**, 441.
Melrose, D. B. (1974b). *Solar Phys.* **37**, 317.
Melrose, D. B. (1975a). *Solar Phys.* **43**, 79.
Melrose, D. B. (1975b). *Solar Phys.* **43**, 211.
Robinson, R. D. (1974). *Proc. Astron. Soc. Aust.* **2**, 258.
Robinson, R. D. (1977). Ph.D. Dissertation, University of Colorado.
Robinson, R. D. (1978a). *Astrophys. J.* **222**, 696.
Robinson, R. D. (1978b). *Aust. J. Phys.* **31**, 547.
Robinson, R. D. (1978c). *Solar Phys.* **56**, 405.
Robinson, R. D., and Smerd, S. F. (1975). *Proc. Astron. Soc. Aust.* **2**, 374.
Rosenberg, H. (1970). *Astron. Astrophys.* **9**, 159.
Sheridan, K. V., Labrum, N. R., and Payten, W. J. (1972). *Nature* **238**, 118.
Tsytovich, V. N. (1967). *Sov. Phys. Usp.* **9**, 805.
Tsytovich, V. N. (1970). 'Non-linear Effects in Plasmas' (Plenum: New York).
Weiss, A. A., and Stewart, R. T. (1965). *Aust. J. Phys.* **18**, 143.
Wild, J. P. (1970). *Proc. Astron. Soc. Aust.* **1**, 365.